Frequency Dependent Switching Characteristics of Back Illuminated OPFET using Finite Difference Methods

Rajesh B. Lohani
Dept of Electronics and Telecommunication
Goa College of Engineering
Farmagudi, Ponda, Goa-India

Jaya V. Gaitonde
Dept of Electronics and Telecommunication
Goa College of Engineering
Farmagudi, Ponda, Goa-India

ABSTRACT
OPFET (Optical Field Effect Transistor) is a useful device for optical communication and as photo detector. In this paper, the switching characteristics of the back illuminated OPFET are plotted using finite difference methods by solving the without time dependent continuity equations in which the incident radiation is allowed to enter through the substrate by inserting a fiber partially into the substrate. The switching parameters include transconductance, channel conductance, drain to source resistance, gate to source, gate to drain and drain to source capacitances.

General Terms
Performance, Theory.

Keywords
OPFET, photodetector, finite-difference methods, back illumination.

1. INTRODUCTION
Over the years, considerable interest has been shown in studying and modeling Optically Controlled Field Effect Transistors (OPFET's) fabricated with Schottky gate configuration. These OPFET's are expected to emerge as promising detectors for use in integrated optoelectronic circuits. A number of theoretical and experimental investigations on the effect of illumination on MESFET structures have been reported [1]-[8].

The switching characteristics of front illuminated OPFET under d. c. condition using analytical methods have been reported [9]. The gate to source capacitance of front illuminated OPFET under a. c. condition has been obtained using perturbation methods [10]. Work has been done on back illuminated OPFET to obtain the I-V characteristics under a. c. conditions using analytical methods as well as numerical methods [11],[12]. The a .c. transconductance and channel conductance of the back illuminated device have been obtained using both the above methods. However, the remaining switching parameters have not been obtained under a. c. conditions numerically. In this paper, finite difference methods are used to obtain the frequency dependent switching characteristics of the back illuminated OPFET.

2. THEORY
The schematic structure of the ion-implanted GaAs OPFET with back illumination is shown in figure 1, having the fiber inserted partially into the substrate so that the absorption takes place in both substrate and active region. The drain-source current flows along the x-direction and the illumination is incident along the y-direction of the device. Electron-hole pairs are generated due to absorption of photons in the neutral substrate region, the

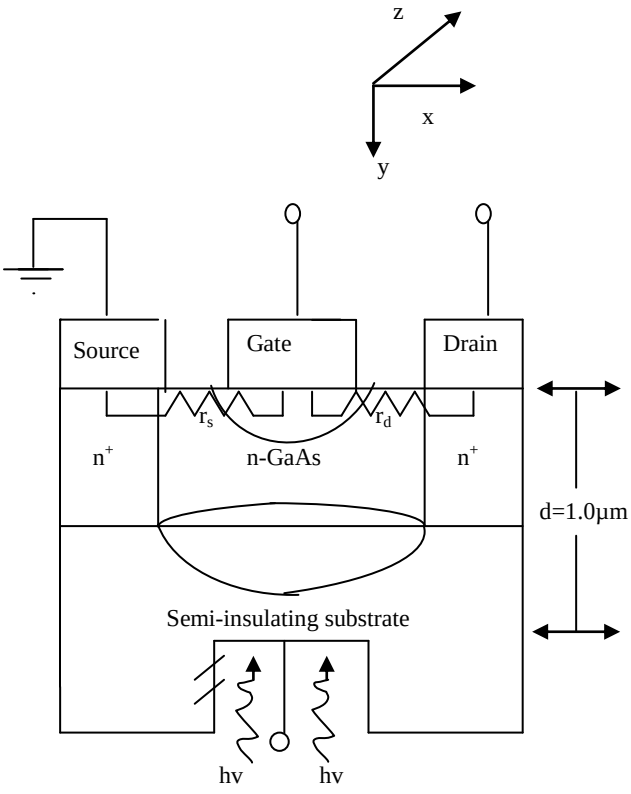

Fig 1: Schematic structure of the device with fiber inserted partially into the substrate [11].

active layer-substrate depletion region, the neutral channel region and the Schottky junction depletion region. The optically generated electrons move toward the channel and contribute to the drain-source current when a drain-source voltage is applied while the holes move in the opposite direction. When these holes cross the junction a photovoltage is developed. This voltage being forward biased reduces the depletion width of both the junctions [11].

In the device, there are four regions namely the neutral channel region, the neutral substrate region, the Schottky junction depletion region and the active layer-substrate depletion region. In the neutral region, the transport

mechanism of carriers is due to diffusion and recombination. So the continuity equation is represented by a second order differential equation.

The frequency dependent equation is given by [11]

$$\frac{\partial^2 n}{\partial y^2} - \frac{n}{D_n \tau_{\omega n}} = -\frac{\alpha \phi_1 e^{-\alpha(d-y)}}{D_n} \quad (1)$$

where n is the number of electrons, D_n is the diffusion constant for electrons, $\tau_{\omega n}$ is the frequency dependent lifetime of electrons, α is the absorption coefficient, Φ_1 is the a. c. part of the radiation flux density, d is the surface to substrate thickness and y is the distance from surface towards the substrate. The term $\Phi_1 e^{-\alpha(d-y)}$ represents the generation rate.

$\tau_{\omega n}$ is given by [11]

$$\frac{1}{\tau_{\omega n}} = \frac{1}{\tau_n} + j\omega \quad (2)$$

where τ_n is the lifetime of the electrons and ω is the frequency.

First we consider neutral channel region. The effect of surface recombination is not present in case of electrons since only the presence of negative traps has been assumed at or close to the surface.

Substituting the finite difference approximation for the second order partial derivative and for the term $e^{-\alpha(d-y)}$ in equation (1), the following equation is obtained:

$$\frac{n_{i+1} - 2n_i + n_{i-1}}{\Delta y^2} - \frac{n_i}{D_n \tau_{\omega n_i}} = -\frac{\alpha \phi_1 e^{-\alpha d}\left(e^{\alpha y_i + \alpha \Delta y/2} - e^{\alpha y_i - \alpha \Delta y/2}\right)}{D_n} \quad (3)$$

The above equation can be written as

$$D_n \tau_{\omega n_i}[n_{i+1} - 2n_i + n_{i-1}] - \Delta y^2 [n_i] = -\alpha \phi_1 e^{-\alpha d} \Delta y^2 \tau_{\omega n_i}\left(e^{\alpha y_i + \alpha \Delta y/2} - e^{\alpha y_i - \alpha \Delta y/2}\right) \quad (4)$$

For m number of finite difference points, i=2 to m-1 is substituted in equation (16), so that m-2 equations with m unknowns are obtained. So the boundary conditions are used to know 2 out of the m unknowns. The boundary conditions are

At $y=y_{dg1}$,

$$n = \alpha \phi_1 \tau_{\omega n} e^{-\alpha(d - y_{dg1})} \quad (5)$$

and at $y=y_{ds1}$,

$$n = \alpha \phi_1 \tau_{\omega n} e^{-\alpha(d - y_{ds1})} \quad (6)$$

where d is the surface to substrate thickness, $\tau_{\omega n}$ is the lifetime of the electrons under ac condition, y_{dg1} is the extension of the Schottky junction depletion region in the channel measured from the surface and y_{ds1} is the extension of the p-n junction depletion region in the channel measured from the surface.

y_{dg1} is given as [11]

$$y_{dg1} = \left[\frac{2\varepsilon}{qN_{dr}}(\phi_B - \Delta + v(x) - v_{gs} - V_{OP1})\right]^{\frac{1}{2}} \quad (7)$$

assuming the abrupt junction approximation where N_{dr} is the equivalent constant doping concentration, Φ_B is the Schottky barrier height, Δ is the position of Fermi level below the conduction band, v(x) is the voltage drop beneath the gate which varies from 0 at the source end and V_{ds} at the drain end. V_{ds} is the drain to source voltage and v_{gs} is the gate to source voltage. V_{OP1} is the photovoltage across the Schottky junction.

y_{ds1} is given as [11]

$$y_{ds1} = a - \frac{N_A}{N_{dr}}\left[\frac{2\varepsilon}{qN_A}(v_{bi} + v(x) - v_{bs} - V_{OP2})\right]^{\frac{1}{2}} \quad (8)$$

assuming abrupt junction approximation where N_A is the substrate doping concentration, v_{bi} is the built-in potential, v_{bs} is the substrate potential and V_{OP2} is the photovoltage across the channel-substrate junction.

V_{OP1} and V_{OP2} are calculated as follows:

The external photovoltage V_{OP1} across the Schottky junction is calculated using the relation [11]

$$V_{OP1} = \frac{kT}{q}\ln\left(\frac{J_p}{J_s}\right) = \frac{kT}{q}\ln\left(\frac{qv_y p(0)}{J_{s1}}\right) \quad (9)$$

where J_{s1} is the reverse saturation current density across the Schottky junction. p(0) is the number of holes crossing the junction at y=0. k is the Boltzmann constant, T is the absolute temperature and q is the electronic charge.

The internal photovoltage V_{OP2} across the channel-substrate junction is obtained using the relation [11]

$$V_{OP2} = \frac{kT}{q}\ln\left(\frac{J_p(a)}{J_{s2}}\right) = \frac{kT}{q}\ln\left(\frac{qv_y p(a)}{J_{s2}}\right) \quad (10)$$

where J_{s2} is the reverse saturation current density for the p-n junction. p(a) is the number of holes crossing the junction at y=a, a is the active layer thickness. p(0) and p(a) is obtained by solving the continuity equation for holes in the Schottky junction depletion region and the channel-substrate depletion region respectively.

Table 1. Values of different parameters used for calculation

Parameter	Name	Value	Unit	Ref.
σ	Straggle Parameter	$0.383x10^{-7}$	(m)	[11]
R_p	Projected Range	$0.861x10^{-7}$	(m)	[11]
μ_n	Electron mobility	0.85	(m^2/V.s)	[9]
Z	Channel Width	$100x10^{-6}$	(m)	[11]
α	Absorption Coefficient	$1.0x10^{6}$	(m^{-1})	[11]
τ_n	Electron Lifetime	$1.0x10^{-6}$	(s)	[11]
τ_p	Hole Lifetime	$1.0x10^{-8}$	(s)	[11]
v_y	Carrier Velocity in y direction	$1.2x10^{5}$	(m/s)	[11]
d	Thickness of the device including substrate	$1.0x10^{-6}$	(m)	[11]
L	Channel Length	$3.0x10^{-6}$	(m)	[11]
a	Active Layer Thickness	$0.25x10^{-6}$	(m)	[11]
Δ	Position of Fermi Level below the conduction band	0.02	(eV)	[11]
Φ_B	Schottky Barrier Height	0.9	(eV)	[11]
N_T	Trap Density	$4.0x10^{17}$	(m^{-2})	[9]
k_p	Capture factor for holes	$3.1x10^{-17}$	(m^3/s)	[11]
k_n	Capture factor for electrons	$3.1x10^{-15}$	(m^3/s)	[11]
v_{bs}	Substrate potential	0.0	(V)	[11]
N_A	Substrate doping concentration	$1.0x10^{20}$	(m^{-3})	[11]
N_{dr}	Equivalent constant doping concentration	$0.658x10^{23}$	(m^{-3})	[11]

Table 1 shows the values of different parameters used in calculation.

Now by substituting the boundary conditions, m-2 equations with m-2 unknowns are obtained.

These equations are solved by writing the coefficients of the unknowns in a matrix. It will be a (m-2)x(m-2) matrix. This matrix will be multiplied by the (m-2)x1 matrix of the unknowns n2 to nm-2. This will be the left hand side of the equation. The right hand side will be the (m-2)x1 matrix consisting of the values obtained from the remaining terms. Now using matrix inversion we will get the values of n. Then the boundary values are appended to the values n_2 to n_{m-2}. This is done for all the boundaries obtained by taking each value of y_{dg1} and y_{ds1}.

Now, these values of n are used to calculate the amount of charge in the neutral channel region which is the integration or summation of number of electrons in each space step multiplied by the electronic charge. It is given as

$$Q_{ch} = q[n_1\Delta y + n_2\Delta y + n_3\Delta y + ... + n_m\Delta y] \quad (11)$$

This is done for each pair of boundaries.

The current in the neutral channel region is given by [11]

$$I_{ch} = \frac{\mu Z}{L}\int_0^{V_{ds}} Q_{ch}\,dv \qquad (12)$$

where V_{ds} is the drain to source voltage, μ is the mobility of electrons, Z is the channel width and L is the channel length. Here the limits of integration are: 0 as the lower limit and V_{ds} as the upper limit. We use summation to calculate the current since the discrete equivalent of integration is summation. The limits 0 and V_{ds} is the voltage v(x) beneath the gate which varies as 0 at the source end and V_{ds} at the drain end. For m finite difference points there will be m values of the voltage v(x). The value obtained by taking the difference between any two consecutive values is dv. This is the voltage drop beneath the gate as we go from source to drain. Then we start from the source end and calculate the value of charge between the first pair of boundaries from equation (20). Then we multiply this value of charge with the first voltage drop at the source end. Then we calculate the value of charge between the second pair of boundaries from equation (20). Then we multiply this value of charge with the second voltage drop. Similarly we repeat this procedure for the other pair of boundaries till we reach the m^{th} pair of boundaries. Then we add all the values and multiply the resulting value with μZ/L to obtain the value of channel current for the corresponding value of V_{ds}. Since we vary V_{ds} between 0 to V volts taking m number of points, the value of channel current is calculated for each value of V_{ds}. So, we get m values of channel current for m values of V_{ds}.

The drain to source current due to photogeneration in the neutral substrate region, the Schottky junction depletion region and the active-layer substrate region and due to ion implantation is calculated as in [12].

The ac component of the total drain-source current is contributed by the carriers due to ion-implantation and optical generation in the channel and substrate regions. It can be represented as [11]

$$I_{ds}(total) = I_{ion} + I_{ch} + I_{dep} + I_{sub} \qquad (13)$$

where I_{ion} is the current due to ion implantation. I_{ch} and I_{sub} are the currents obtained in the neutral channel and neutral substrate regions respectively and I_{dep} is the current obtained in the Schottky junction depletion region and active layer-substrate depletion region due to optical generation.

From the drain to source current, the channel charge, the charge in the Schottky junction depletion region, the gate to source voltage and the drain to source voltage, the parameters transconductance, channel conductance, the drain to source resistance and the capacitances are obtained.

The finite difference calculation of transconductance g_m is given as [13]

$$g_m\{v_{gs}(i)\} = \frac{I_{ds}(i+1) - I_{ds}(i-1)}{v_{gs}(i+1) - v_{gs}(i-1)} \quad (14)$$

and the finite difference calculation of gate to source capacitance C_{gs} is given as [13]

$$C_{gs}\{v_{gs}(i)\} = \frac{Q_{d1}(i+1) - Q_{d1}(i-1)}{v_{gs}(i+1) - v_{gs}(i-1)} \quad (15)$$

where I_{ds} is the drain to source current, v_{gs} is the gate to source voltage and Q_{d1} is the charge in the Schottky junction depletion region. $I_{ds}(j)$, $v_{gs}(j)$ and $Q_d(j)$ are the values of the corresponding parameters at the j^{th} step. In both the above formulae the drain to source voltage V_{ds} is kept constant.

The finite difference calculation of channel conductance g_d, drain to source resistance R_{ds}, gate to drain capacitance C_{gd} and drain to source capacitance C_{ds} is given as follows:

$$g_d\{V_{ds}(i)\} = \frac{I_{ds}(i+1) - I_{ds}(i-1)}{V_{ds}(i+1) - V_{ds}(i-1)} \quad (16)$$

$$R_{ds}\{V_{ds}(i)\} = \frac{V_{ds}(i+1) - V_{ds}(i-1)}{I_{ds}(i+1) - I_{ds}(i-1)} \quad (17)$$

$$C_{gd}\{V_{ds}(i)\} = \frac{Q_{d1}(i+1) - Q_{d1}(i-1)}{V_{ds}(i+1) - V_{ds}(i-1)} \quad (18)$$

$$C_{ds}\{V_{ds}(i)\} = \frac{Q_{d2}(i+1) - Q_{d2}(i-1)}{V_{ds}(i+1) - V_{ds}(i-1)} \quad (19)$$

where V_{ds} is the drain to source voltage and Q_{d2} is the channel charge. $V_{ds}(j)$, $Q_{d2}(j)$ and $I_{ds}(j)$ are the values of the corresponding parameters at the j^{th} step. In the above formulae, v_{gs} is kept constant.

3. RESULTS AND DISCUSSIONS

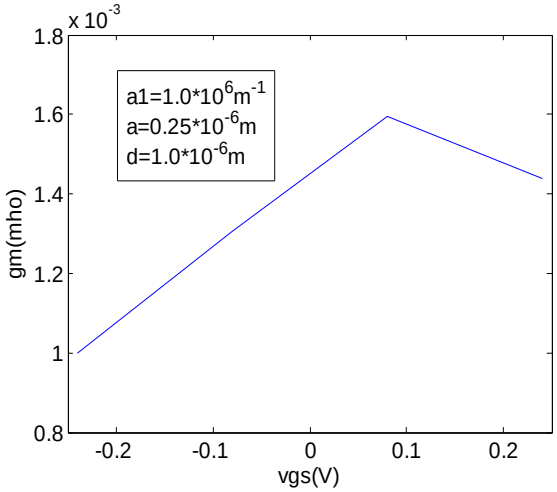

Fig 2: Transconductance v/s gate to source voltage.

Figure 2 shows the plot of transconductance versus gate to source voltage. The transconductance is an important parameter which determines the maximum cut-off frequency of the operation of the device. It is seen that initially with the increase in the gate to source voltage the transconductance increases gradually and reaches a peak. With the further increase in the gate to source voltage the transconductance decreases steadily. It is because at positive gate voltages some of the electrons are attracted toward the gate instead of reaching the drain. Also the holes which where crossing the Schottky junction gets repelled and decreases. So the cumulative effect of the above two phenomena causes the decrease in the transconductance.

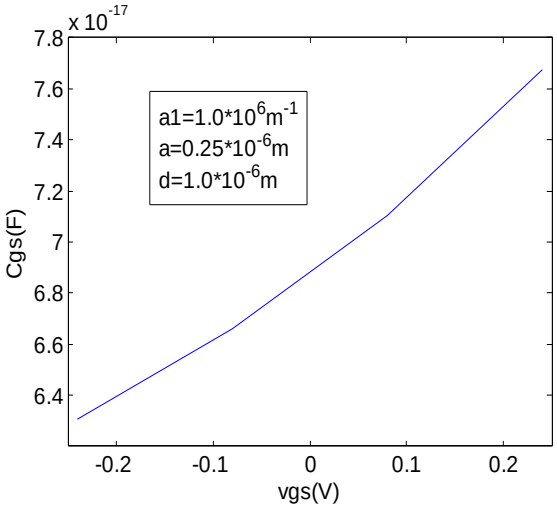

Fig 3: Gate to source capacitance v/s gate to source voltage.

Figure 3 shows the plot of gate to source capacitance versus gate to source voltage. It is seen that with the increase in the gate to source voltage, the capacitance increases. With the increase in the gate to source voltage, the change in the depletion width below the gate increases. This results in the greater increase in the change in the charge below the gate. This increases the capacitance.

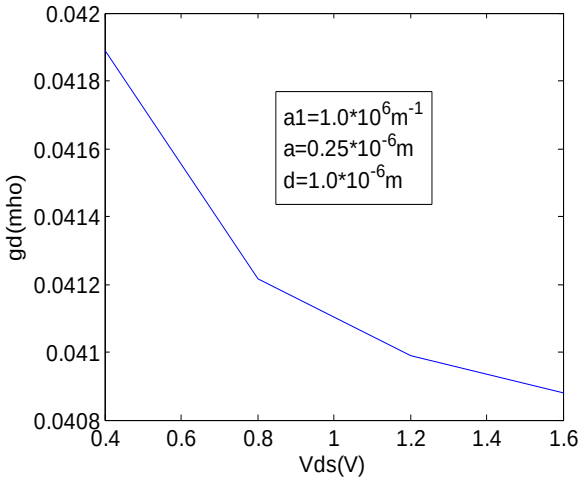

Fig 4: Channel conductance v/s drain to source voltage.

Figure 4 shows the plot of channel conductance versus drain to source voltage. It is seen that with the increase in the drain to source voltage, the channel conductance decreases. With the increase in the drain to source voltage, the change in the depletion width below the gate and the width measured from the surface to the active layer-substrate depletion region extension in the channel decreases. This decreases the change in the current with respect to the change in the voltage which in turn decreases the channel conductance.

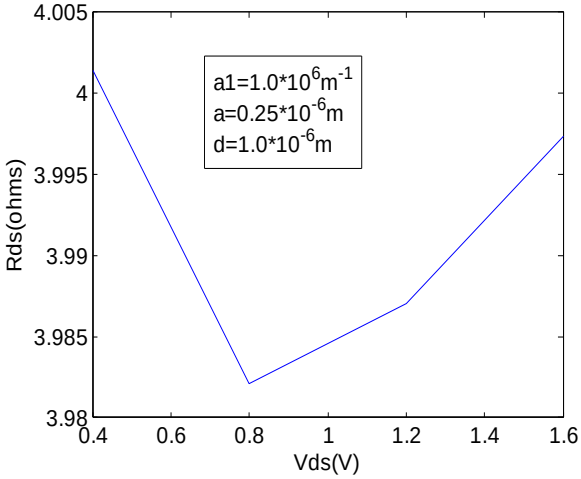

Fig 5: Drain to source resistance v/s drain to source voltage.

Figure 5 shows the plot of drain to source resistance versus drain to source voltage. It is seen that with the increase in the drain to source voltage from 0.4V to 0.8V the drain to source resistance decreases, while further increase in the drain to source voltage increases the resistance. At lower voltages the effective channel width is more, so resistance is less. As voltage is increased, the channel begins to constrict and the resistance increases.

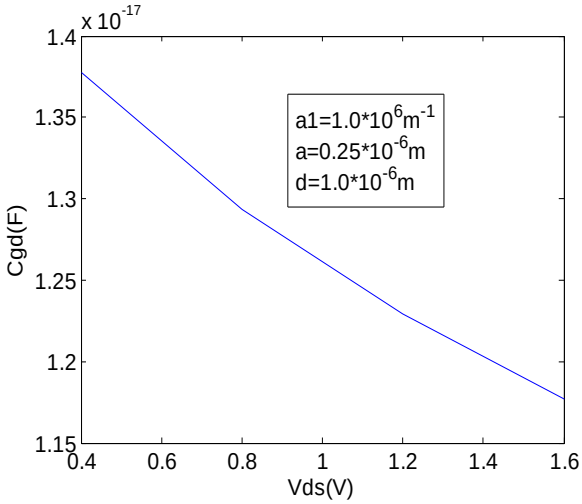

Fig 6: Gate to drain capacitance v/s drain to source voltage.

Figure 6 shows the plot of gate to drain capacitance versus drain to source voltage. It is seen that with the increase in the drain to source voltage, the capacitance decreases. With the increase in the drain to source voltage, the change in the depletion width below the gate decreases. This decreases the change in the charge below the gate which in turn decreases the capacitance.

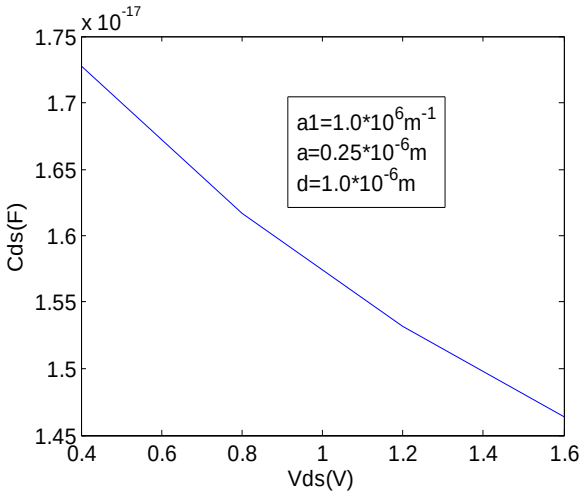

Fig 7: Drain to source capacitance v/s drain to source voltage.

Figure 7 shows the plot of drain to source capacitance versus drain to source voltage. It is seen that with the increase in the drain to source voltage, the capacitance decreases. With the increase in the drain to source voltage, the change in the depletion width below the gate and the width measured from the surface to the active layer-substrate depletion region extension in the channel decreases. This decreases the change in the effective channel width. This decreases the change in the channel charge. Hence the capacitance decreases.

4. CONCLUSION

The continuity equation for electrons has been solved and switching parameters have been obtained using finite difference methods. The results obtained agree with the reported literature. This shows the accuracy of finite difference methods. Better performance is obtained with back illumination than the reported work with front illumination [9]. Higher values of transconductance and channel conductance and low values of gate to source capacitance, gate to drain capacitance, drain to source capacitance and drain to source resistance indicate that the back illuminated device is a potential candidate for switching.

5. ACKNOWLEDGEMENT

Authors thanks Dr. B.B. Pal , ITBHU and Dr. R. P. R. C. Aiyar, IIT, Mumbai for providing constant help and encouragement and necessary guidance.

6. REFERENCES

[1] H. Mizuno, "Microwave characteristics of an optically controlled GaAs-MESFET", IEEE Trans. Microwave Theory Tech., Vol. MlT-31, pp. 59&600, 1983.

[2] A. A. De Salles, "Optical control of GaAs MESFET's", IEEE Trans. Microwave Theory Tech., Vol. MTT-31, pp. 812-820, 1983.

[3] J. L. Cantier, D. Pasqwt, and P. Ponvil, "Optical effects on the static and dynamic characteristics of GaAs-MESFET", IEEE Trans. Microwave Theory Tech., Vol. MTT-33, pp. 819-822, 1985.

[4] R N. Simons and K. B. Bhasin, "Analysis of optically controlled microwave/millimeter wave device structure", IEEE Trans. Microwave Theory Tech., Vol. MTT-34, pp. 1349-1355, 1986.

[5] R N. Simons, ''Microwave performance of an optically controlled AlGaAs/GaAs high electron mobility transistor and GaAs MESFET", IEEE Trans. Microwave Theory Tech., Vol. MTT-35, pp. 1444-1455, 1987.

[6] R. B. Darling and J. P. Uyemura, "Optical gain and large-signal characteristics of illuminated GaAs MESFET's", IEEE J. Quantum Electron, Vol. QE-23, pp. 1160-1171, 1987.

[7] Sunita Mishra, V. K. Singh and B. B. Pal, "Effect of Radiation and Surface Recombination on the Characteristics of an Ion-Implanted GaAs MESFET", IEEE Transactions on Electron Devices, Vol. 37, No. 1, pp. 2-10, January 1990.

[8] P. Chakrabarti, N. L. Shrestha, S. Srivastava, and V. Khemka, "An improved model of an ion-implanted GaAs OPFET", IEEE Transactions on Electron Devices, Vol. 39, pp. 2050-2059, 1992.

[9] P. Chakrabarti, S. K. Shrestha, A. Srivastava, and D. Saxena, "Switching characteristics of an optically controlled GaAs-MESFET", IEEE Trans. Microwave Theory Tech., Vol. 42, No. 3, March 1994.

[10] Youssef Zebda and S. Abu_Helweh, "AC Characteristics of Optically Controlled MESFET (OPFET)", Journal of Lightwave Technology, Vol. 15, No. 7, pp. 1205-1212, July 1997.

[11] Nandita Saha Roy and B. B. Pal, "Frequency-Dependent OPFET Characteristics with Improved Absorption under Back Illumination", Journal of Lightwave Technology, Vol. 18, No. 4, pp. 604-613, April 2000.

[12] Rajesh B. Lohani and Jaya V. Gaitonde, "I-V and switching characteristics of back illuminated OPFET using finite difference methods", International Journal of Computer Applications (0975 – 8887), Vol. 31, No. 4, pp. 5-11, October 2011.

[13] P. Chakrabarti, M. Madheswaran, A. Gupta and N. A. Khan, "Numerical Simulation of an Ion-Implanted GaAs OPFET", IEEE Transactions on Microwave Theory and Techniques, Vol. 46, No. 10, pp. 1360-1366, October 1998.